Replication dynamics in fission and budding yeasts through DNA polymerase tracking

*Enrique Vázquez and Francisco Antequera**

The dynamics of eukaryotic DNA polymerases has been difficult to establish because of the difficulty of tracking them along the chromosomes during DNA replication. Recent work has addressed this problem in the yeasts *Schizosaccharomyces pombe* and *Saccharomyces cerevisiae* through the engineering of replicative polymerases to render them prone to incorporating ribonucleotides at high rates. Their use as tracers of the passage of each polymerase has provided a picture of unprecedented resolution of the organization of replicons and replication origins in the two yeasts and has uncovered important differences between them. Additional studies have found an overlapping distribution of DNA polymorphisms and the junctions of Okazaki fragments along mononucleosomal DNA. This sequence instability is caused by the premature release of polymerase δ and the retention of non proof-read DNA tracts replicated by polymerase α. The possible implementation of these new experimental approaches in multicellular organisms opens the door to the analysis of replication dynamics under a broad range of genetic backgrounds and physiological or pathological conditions.

DOI 10.1002/bies.201500072

Instituto de Biología, Funcional y Genómica (IBFG), Consejo Superior de Investigaciones Científicas (CSIC), Universidad de Salamanca, Campus Miguel de Unamuno, Salamanca, Spain

***Corresponding author:**
Francisco Antequera
E-mail: cpg@usal.es

Abbreviations:
dNTPs, deoxyribonucleotides; **ORC,** origin recognition complex; **ORI,** origin of replication; **rNTPs,** ribonucleotides; **SNP,** single nucleotide polymorphism.

Keywords:
DNA polymerases; DNA replication; replication origin; genome instability; nucleosomes

Introduction

In eukaryotes, the initiation of DNA replication depends on the progressive assembly of specialized protein complexes on multiple replication origins (ORI) along chromosomes. The activation of these complexes triggers the S phase of the cell cycle by initiating the divergent and bidirectional synthesis of new DNA daughter strands by DNA polymerases, which proceed until replicons moving in opposite directions converge and fuse to generate a fully replicated genome.

Many of the essential molecules involved in this process have been conserved along evolution and the basic biochemical steps of DNA replication are well established [1, 2]. The recent development of in vitro systems capable of sustaining plasmid replication [3, 4] and the reconstitution of replication forks using purified proteins [5, 6] will facilitate further dissection of the molecular mechanisms driving replication initiation.

Contrary to the conservation of replication proteins, ORI sequences have diversified considerably along evolution. Even in individual genomes, ORIs show a very high level of sequence degeneracy, making it impossible to identify them on the basis of the sequence alone. The absence of conserved sequence elements has led to the exploitation of different biochemical features of replication with a view to map the distribution of ORIs in the genome. As in many other aspects of biology, local approaches to identify ORIs have been replaced by genome-wide methods, for which genome replication is particularly well suited. These strategies have included the localization of binding sites of initiator proteins, the identification of short DNA nascent strands and the incorporation of bromodeoxyuridine to label newly synthesized DNA. The advantages and limitations of such strategies have been discussed in detail [7–9].

Defining the dynamics of eukaryotic DNA polymerases has been hampered by the lack of an efficient system to track their passage along the chromosomes during DNA replication. In this review, we will focus on very recent analyses of replication dynamics in the yeasts *Schizosaccharomyces pombe* and *Saccharomyces cerevisiae*, based on the incorporation of ribonucleotides (rNTPs) in DNA followed by high-throughput sequencing of the trail of rNMPs left behind the passage of the DNA polymerases [10–13]. The combination of these analyses with the interference of nucleosomes in the maturation of Okazaki fragments [14, 15] has uncovered a functional link between DNA replication, the organization of chromatin, and the presence of regions of instability across the genome.

Engineering the incorporation of ribonucleotides in DNA as tracers of the passage of replicative polymerases

The incorporation of nucleotides in the 5′–3′ direction by DNA polymerases implies that the two antiparallel DNA strands must be replicated through different mechanisms. DNA synthesis is initiated by DNA polymerase α (Pol α) [16] whose primase activity synthesizes de novo a short RNA primer that is approximately 8–10 ribonucleotides long and is elongated through the addition of 10–30 deoxyribonucleotides. At this stage, Pol α is replaced by DNA polymerase ε (Pol ε) [17], which catalyzes the synthesis of the continuous daughter strand. On the complementary strand, Pol α is replaced by DNA polymerase δ (Pol δ) [18] to add another 180–200 deoxyribonucleotides. These Okazaki fragments are synthesized opposite to the movement of the replication fork, and they are subsequently processed and ligated to generate the lagging DNA daughter strand [5, 6, 19].

Not surprisingly, DNA polymerases have been selected to favor the incorporation of deoxyribonucleotides (dNTPs) relative to ribonucleotides (rNTPs) against the 36- to 190-fold molar excess of rNTPs relative to dNTPs in the nucleus [20]. Despite this preference, misincorporation of rNTPs is the most common error that occurs during DNA replication and amounts to an estimated 10,000 rNMPs per genome during each round of in vivo replication in *S. cerevisiae* [20] and to over a million in mouse cells [21]. Ribonucleotides are removed from DNA by several mechanisms, of which the ribonucleotide excision repair (RER) pathway is the most efficient [22]. The RNase H2 ribonuclease generates a nick 5′ to the rNMP, which is followed by extension from the free 3′-OH terminus by Pol δ or Pol ε. The displaced strand harboring the rNMP at its 5′ end is removed by the FEN1 or EXO1 nucleases and the remaining nick is sealed by DNA ligase 1 [23]. The decreased removal of rNMPs due to the inactivation of the RNase H2 causes replication stress and genome instability in a wide variety of organisms due to the higher reactivity of the oxygen atom of the ribose [20–22, 24].

Four recent studies have used *S. cerevisiae* and *S. pombe* mutants whose replicative polymerases were engineered by introducing point mutations in their catalytic domains to enhance the misincorporation of rNTPs [10–13]. Additional deletion of the *rnh201* gene encoding the RNase H2 ensured that the rNTPs incorporated were not removed from the DNA, such that the passage of each polymerase along the DNA could be followed by the trail of rNTPs left behind. To identify the sites of rNMP incorporation, purified genomic DNA from exponential cultures was treated either with RNAse H2 and denatured or with alkali to hydrolyze the DNA molecule in the 5′ or 3′ position of the rNMPs, respectively. The resulting single-stranded DNA fragments were size-selected and tagged with short bar-coded adaptors at their rNMP end prior to cloning and high-throughput sequencing. Alignment of the sequence reads to the reference genome identified the position of the rNMP along the two DNA strands in the individual Pol α, δ, and ε mutants and defined which genomic regions were preferentially replicated by each polymerase.

Replicons in *S. pombe* and *S. cerevisiae* have a different structure

The antiparallel organization of the DNA strands predicts that approximately half of the genome should be replicated by Pol δ and half by Pol ε and this is clearly confirmed by the division of labor between the two polymerases shown in Fig. 1. An immediately observable difference between *S. pombe* and *S. cerevisiae* replicons, however, is that the average length of the regions replicated by Pol δ and by Pol ε is smaller in *S. pombe*, implying that the ORI density along the chromosomes is higher than in *S. cerevisiae*.

Because not all replication origins are active in each S phase, their probability of firing is referred to as their "efficiency." This means that the genome of individual cells in the population will be replicated from a different subset of ORIs in any given S phase, and will follow a different replication pattern, as has been shown in DNA-combing analyses [25, 26]. As a consequence, many genomic regions in the population will not appear to be exclusively replicated by Pol ε and Pol δ, but the ratio of use between them will range between 0 and 1. The relative use of each polymerase switches sharply at ORIs and gradually decays from them to converge at a point where the ratio of use of Pol δ and Pol ε approaches 0.5 in regions where the average number of forks moving in opposite directions is the same. This implies that although ORIs map to discrete genomic regions, there are no preferred sites of termination, and that the fusion of converging replicons in individual cells takes place at different inter-origin positions in different cells (Fig. 1). Inflections in the replicon profile (Fig. 2) reflect small-scale switches between Pol δ and Pol ε associated with low-efficiency ORIs firing only in a small fraction of the population. These ORIs are passively replicated in the remaining cells from replicons originated by more efficient ORIs. This phenomenon is also present in *S. cerevisiae* but at a much lower scale (Fig. 2). As discussed in the next section, this is probably due to the different strategy of ORI specification in the two yeasts.

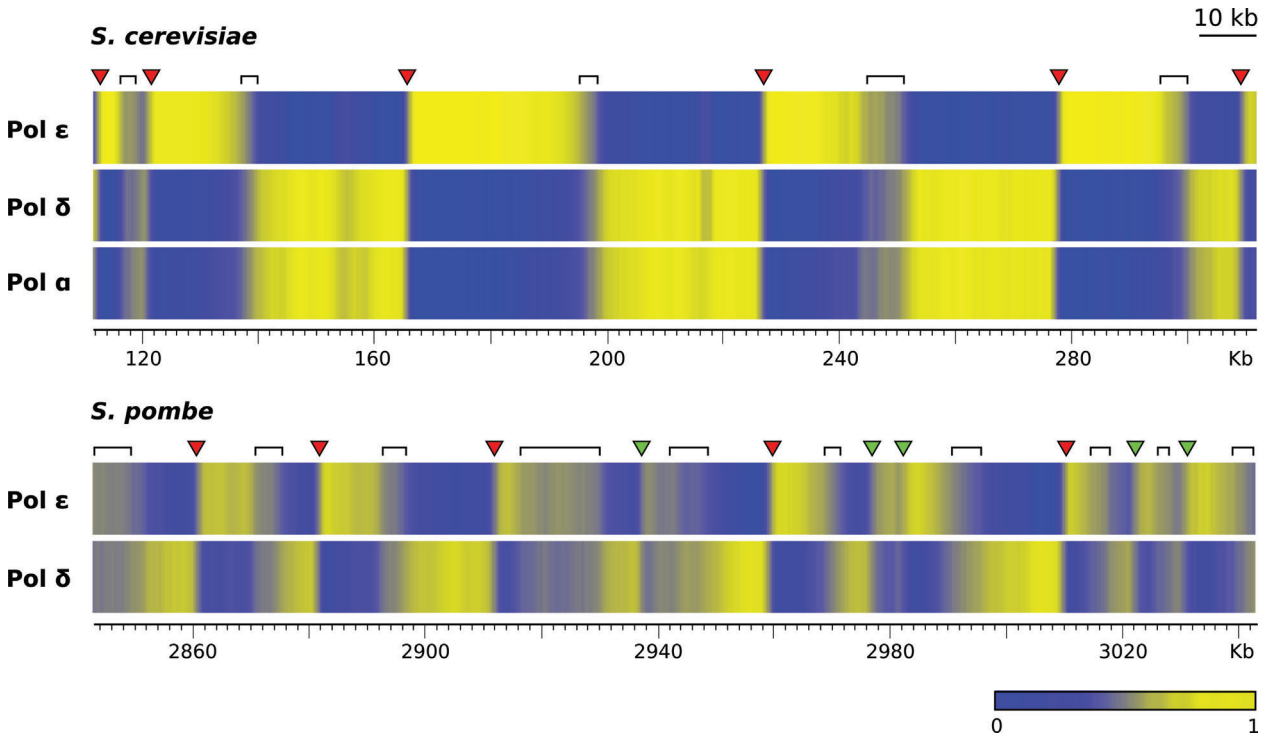

Figure 1. Division of labor between polymerases and replicon sizes in *S. cerevisiae* and *S. pombe*. Heatmaps show the ratio between Pol δ- and Pol ε-synthesized DNA using the bottom (Crick) strand as a template of the indicated genomic regions of chromosomes XV and chromosome I of *S. cerevisiae* and *S. pombe*, respectively. The distribution of Pol α and Pol δ relative to Pol ε coincides along the lagging strand in *S. cerevisiae* (Pol α was not mapped in *S. pombe*). Red arrowheads point to sites of sharp switching between polymerases that coincide with strong replication origins in the two yeasts. Weak ORIs in *S. pombe* are indicated by green arrowheads. Intermediate blue/yellow color (brackets) corresponds to termination zones. Heatmaps were generated from the original sequencing data of Clausen et al. [10] (*S. cerevisiae*) and Daigaku et al. [13] (*S. pombe*).

Origin specification in *S. pombe* and *S. cerevisiae* determines a different replication dynamics

An important feature of the rNTP mapping methodology is that, in addition to localizing ORIs very precisely, it gives a measure of their efficiency by the amplitude of the switch between polymerases (Fig. 3). ORIs in *S. cerevisiae* have a modular structure made up of an 11 bp long ARS consensus element (ACS) that is essential for their activity, and several short and variable auxiliary elements. They have been mapped genome wide by several methods and the efficiency and timing of firing during the S phase has been estimated for many of them [27–31]. Ninety five percent of those ORIs colocalize with sites of polymerase switching and their efficiency is consistent with that previously estimated for some of them by two-dimensional gel electrophoresis [29, 32–35] (Figs. 2 and 3). In addition, the new study by Clausen et al. [10] has identified 72 sites of Pol δ/Pol ε switching, corresponding to previously undetected ORIs in *S. cerevisiae*.

Replication origins in *S. pombe* have a different organization because they lack consensus sequence elements. Their only shared feature is a high A + T content, regardless of the primary DNA sequence [35, 36]. This seems to be their only requirement, as suggested by the finding that artificial A + T-rich DNA fragments of arbitrary sequence can initiate replication in the chromosome as efficiently as endogenous ORIs [34]. As in the case of *S. cerevisiae*, ORIs have been mapped genome wide in *S. pombe* by several methods [26, 35, 37–39] and the large majority of them colocalize with sites of Pol δ/Pol ε switching identified by Daigaku et al. [13]. The efficiency of ORIs as measured by the amplitude of the switch between Pol δ and Pol ε correlates with their A + T content (Fig. 3), as previously found for individual ORIs [34]. This correlation reflects the fact that the origin recognition complex (ORC) is targeted to ORIs in *S. pombe* through the AT-hooks of the Orc4 subunit of the ORC complex [40]. A higher density of ORIs in *S. pombe* is likely due to the presence of A + T-rich sequence tracts at many intergenic regions susceptible to being targeted by the Orc4 protein. The presence of many low-efficiency ORIs in *S. pombe* is probably the reason why the profile of the replicons is more irregular than in *S. cerevisiae* (Fig. 2).

Nucleosome repositioning on the DNA lagging strand compromises genome stability

Another study, not directly related to the tracking of DNA polymerases during replication, found that junctions

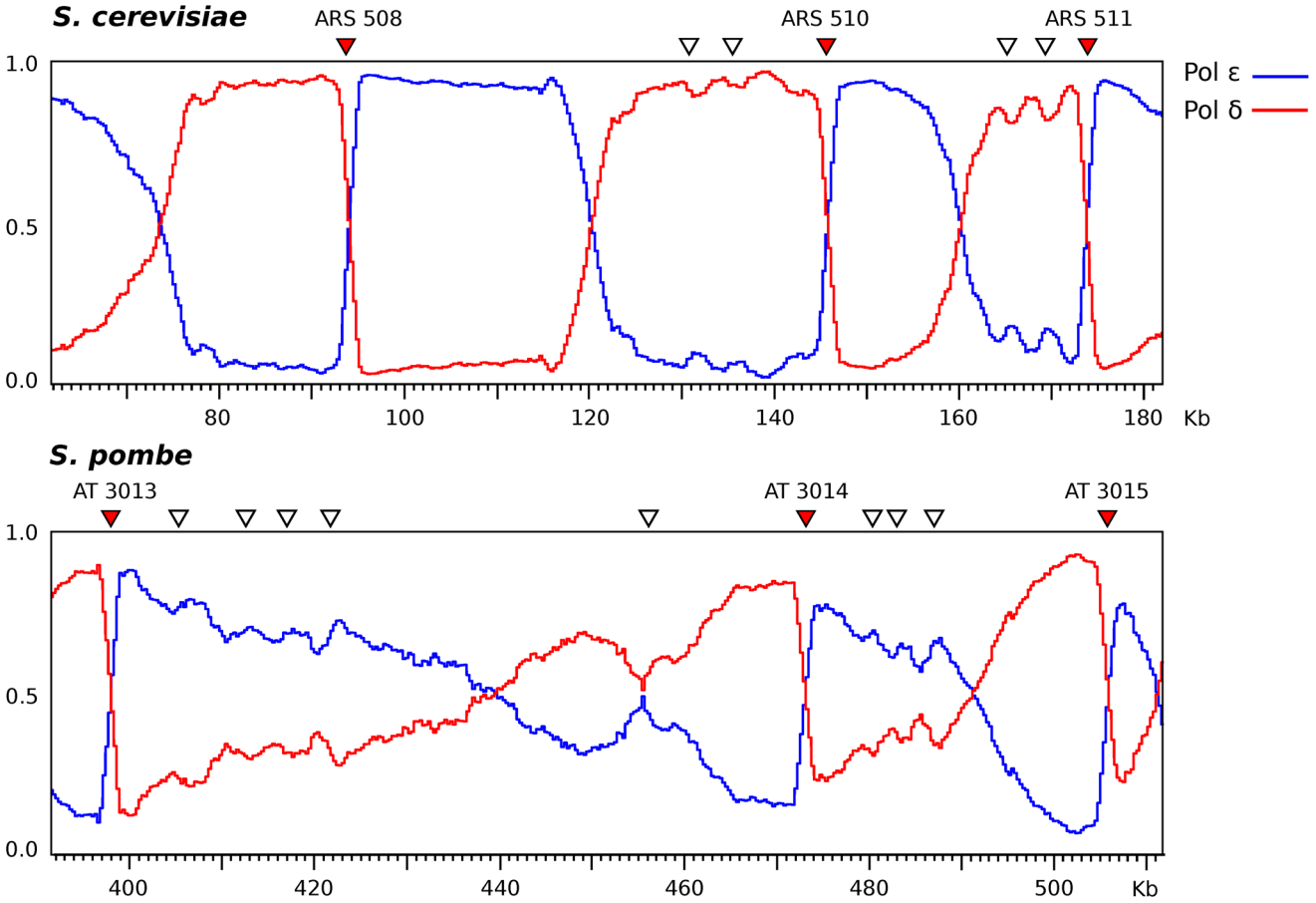

Figure 2. Different replicon structure in *S. cerevisiae* and *S. pombe*. Relative use of Pol δ (red) and Pol ε (blue) along the indicated genomic regions of the bottom (Crick) strand in chromosomes V and III of *S. cerevisiae* and *S. pombe*, respectively. As shown in Fig. 1, termination zones are narrower in *S. cerevisiae* than in *S. pombe*. For example, the 14 and 22 kb of the bottom DNA strand flanking ARS508 in *S. cerevisiae* are replicated almost exclusively by Pol δ and Pol ε, respectively, in most cells in the population. Previously identified early origins ARS508, ARS510, and ARS511 in *S. cerevisiae* and strong origins AT3013, AT3014, and AT3015 in *S. pombe* are indicated by red arrowheads. Inflections in the shape of replicons (white arrowheads) occur more often in *S. pombe* and are probably associated with very weak ORIs, many of which escaped previous detection by other methods.

between Okazaki fragments map preferentially to the central region of the 147 bp of mononucleosomal DNA (nucleosomal dyad) in *S. cerevisiae*. Smith and Whitehouse [14] proposed that the rapid binding of nucleosomes to nascent Okazaki fragments could cause the collision and premature dissociation of the Pol δ engaged in the extension of the next fragment synthesized. The distribution of the nicks at the sites of collision increases towards the dyad region, where the interaction between DNA and the histone core is stronger [41].

Several studies have reported that the frequency of single nucleotide polymorphisms (SNPs) in the nucleosomal dyad region is higher than the genomic average. This feature is present in yeasts and other organisms, including humans, and suggests that different DNA regions around the histone core have a different rate of mutation [42–45]. Following up these observations, Reijns et al. [12] found that the junctions between Okazaki fragments and the previously identified spectrum of SNPs *in S. cerevisiae* largely overlapped along mononucleosomal DNA (Fig. 4). They also used *S. cerevisiae* mutants harboring Pol α, δ, and ε polymerases engineered to incorporate rNTPs in order to test the possibility that the premature release of Pol δ might result in the retention of DNA Pol α-synthesized DNA at the 5′ end of mature Okazaki fragments. Measurement of the incorporation rate of rNTPs in vitro and in vivo by wild-type and mutant DNA polymerases, showed that up to 1.5% of Pol α-synthesized DNA was retained in the fully replicated genome whose sequence stability could be compromised by the lack of 3′ to 5′ proofreading exonuclease activity of Pol α. Since this phenomenon applies to the entire genome, it could account for the increased sequence variability at dyad regions in *S. cerevisiae* [42] and for the higher A + T or G + C content of nucleosomal dyads relative to the genomic averages in *S. pombe* and *S. cerevisiae*, respectively [46–48]. Strikingly, in the case of mononucleosomal DNA from coding regions, these differences in base composition determine a different distribution of amino acids in the two species depending on the position of their corresponding codons relative to the dyad position [48]. In *S. pombe*, higher instability in the dyad region is consistent with the fact that its A + T composition is higher than that of

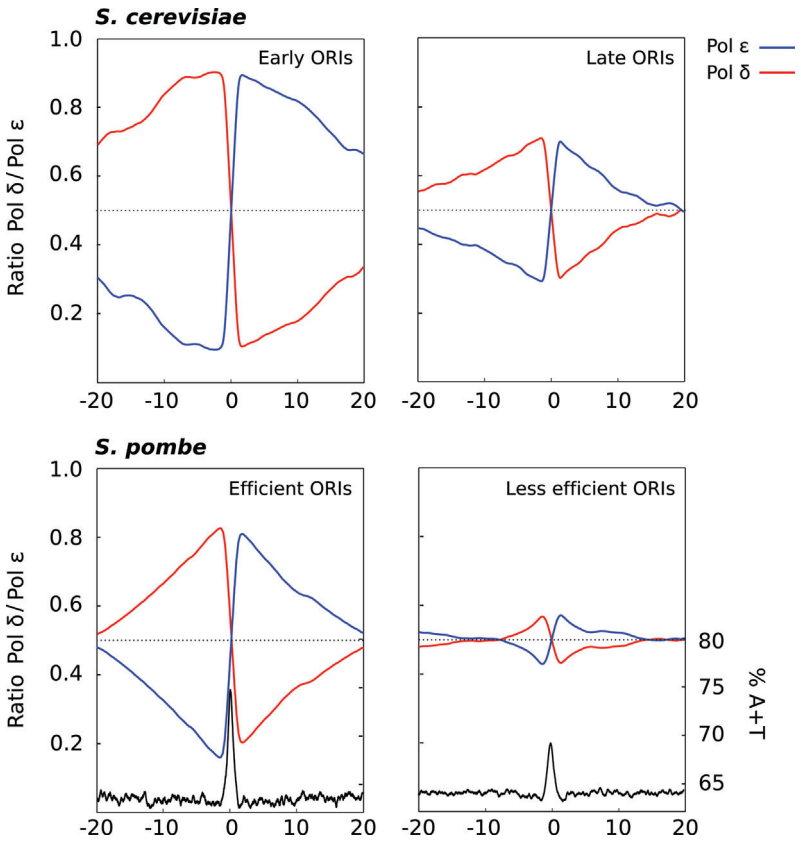

Figure 3. Timing, efficiency, and base composition of replication origins. The replication profiles of genomic regions 40 kb long spanning 100 early and 136 late firing ORIs in *S. cerevisiae* as classified by Soriano et al. [49] were centered on the position of polymerase switching. The amplitude of the switch and the length of the replicons from early ORIs are greater than in late ORIs. In *S. pombe*, ORIs identified by Daigaku et al. [13] were classified according to the amplitude of the switch in two groups of 566 and 579 ORIs of different efficiency. The A + T content (measured in windows of 300 bp and step of 1 bp) is higher in the more efficient ORIs in a region of approximately 2 kb centered on the position of polymerase switching.

the linker DNA [46, 48]. This is probably a consequence of the general bias of the *S. pombe* genome toward increasing its A + T content [36].

The over-representation of Okazaki fragment termini was not limited to nucleosomal dyads but was also detectable at other sites of DNA-protein interaction such as the sites of binding for transcription factors Abf1, Reb1, and Rap1. As in the case of nucleosome assembly on inmature Okazaki fragments, the binding of these proteins to their cognate sites after the passage of the replication fork could affect negatively the processivity of DNA Pol δ [14]. Consistent with this model, the rate of nucleotide substitution is higher in regions immediately adjacent to the binding sites of some regulatory proteins and at the edge of human DNase I footprint regions [12, 14].

Conclusions and outlook

The development of methods to monitor ORI activity and the dynamics of replicons at genome-wide scale in a single experiment represents a turning point in the field of DNA replication. The reliability of these new approaches is supported by the consistency between the replication maps of *S. cerevisiae* generated in two independent laboratories [10, 12] and the coincidence in the localization and efficiency of ORIs with previous analyses in *S. cerevisiae* and *S. pombe*.

At present, precise quantitative analyses of replication are difficult to implement at genome-wide scale and in many cases they can only be applied to individual ORIs. The new qualitative and quantitative analyses of DNA replication will provide a picture of the replication landscape with a

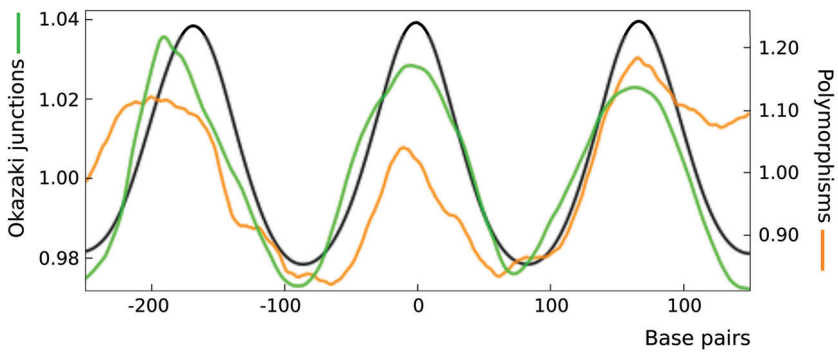

Figure 4. Phased profiles of nucleosomal occupancy, single nucleotide polymorphisms and junctions of Okazaki fragments. The profile of nucleosome occupancy of 3,742 regions 500 bp long spanning three adjacent nucleosomes in the *S. cerevisiae* genome (taken from Quintales et al. [48]) were aligned to the dyad position of the central nucleosome to generate the aggregated profile shown in black. The normalized distribution of polymorphisms [12] (orange) and of the 5′ end of Okazaki fragments [14] (green) on the two DNA strands are in phase with the nucleosomal profile.

resolution comparable to that afforded by RNA-Seq analyses for transcription. For example, this technology will make it possible to monitor the dynamics of replication in different genetic backgrounds and physiological conditions and to assess the impact of stress and physical or chemical challenges on the replication program in vivo. It also opens the possibility of modifying the many non-replicative polymerases present in eukaryotes to track their activity and specificity in maintaining genome integrity. Finally, although the required genetic manipulations will not be as straightforward as in yeasts, the implementation of these methods in multicellular organisms would contribute to defining the replication program in different cell types and to detecting abnormal or unscheduled replication patterns under pathological conditions.

Acknowledgment

This work was funded by the Spanish Ministerio de Economía y Competitividad, grant nos. BFU2011-28804 and BFU2014-52143-P.

The authors declare no conflict of interests.

References

1. **Onesti S, MacNeill SA**. 2013. Structure and evolutionary origins of the CMG complex. *Chromosoma* **122**: 47–53.
2. **O'Donnell M, Langston L, Stillman B**. 2013. Principles and concepts of DNA replication in bacteria, archaea, and eukarya. *Cold Spring Harb Perspect Biol* **5**: a010108.
3. **On KF, Beuron F, Frith D, Snijders AP**, et al. 2014. Prereplicative complexes assembled in vitro support origin-dependent and independent DNA replication. *EMBO J* **33**: 605–20.
4. **Gros J, Devbhandari S, Remus D**. 2014. Origin plasticity during budding yeast DNA replication in vitro. *EMBO J* **33**: 621–36.
5. **Yeeles JTP, Deegan TD, Janska A, Early A**, et al. 2015. Regulated eukaryotic DNA replication origin firing with purified proteins. *Nature* **519**: 431–5.
6. **Georgescu RE, Langston L, Yao NY, Yurieva O**, et al. 2014. Mechanism of asymmetric polymerase assembly at the eukaryotic replication fork. *Nat Struct Mol Biol* **21**: 664–70.
7. **Gilbert DM**. 2010. Evaluating genome-scale approaches to eukaryotic DNA replication. *Nat Rev Genet* **11**: 673–84.
8. **Hyrien O**. 2015. Peaks cloaked in the mist: the landscape of mammalian replication origins. *J Cell Biol* **208**: 147–60.
9. **Urban JM, Foulk MS, Casella C, Gerbi SA**. 2015. The hunt for origins of DNA replication in multicellular eukaryotes. *F1000Prime Rep* **7**: 30.
10. **Clausen AR, Lujan SA, Burkholder AB, Orebaugh CD**, et al. 2015. Tracking replication enzymology in vivo by genome-wide mapping of ribonucleotide incorporation. *Nat Struct Mol Biol* **22**: 185–91.
11. **Koh KD, Balachander S, Hesselberth JR, Storici F**. 2015. Ribose-seq: global mapping of ribonucleotides embedded in genomic DNA. *Nat Methods* **12**: 251–7.
12. **Reijns MAM, Kemp H, Ding J, de Procé SM**, et al. 2015. Lagging-strand replication shapes the mutational landscape of the genome. *Nature* **518**: 502–6.
13. **Daigaku Y, Keszthelyi A, Müller CA, Miyabe I**, et al. 2015. A global profile of replicative polymerase usage. *Nat Struct Mol Biol* **22**: 192–8.
14. **Smith DJ, Whitehouse I**. 2012. Intrinsic coupling of lagging-strand synthesis to chromatin assembly. *Nature* **483**: 434–8.
15. **McGuffee SR, Smith DJ, Whitehouse I**. 2013. Quantitative, genome-wide analysis of eukaryotic replication initiation and termination. *Mol Cell* **50**: 123–35.
16. **Johnson LM, Snyder M, Chang LMS, Davis RW**, et al. 1985. Isolation of the gene encoding yeast DNA polymerase I. *Cell* **43**: 369–77.
17. **Morrison A, Araki H, Clark AB, Hamatake RK**, et al. 1990. A third essential DNA polymerase in *S. cerevisiae*. *Cell* **62**: 1143–51.
18. **Sitney KC, Budd ME, Campbell JL**. 1989. DNA polymerase III, a second essential DNA polymerase, is encoded by the *S. cerevisiae* CDC2 gene. *Cell* **56**: 599–605.
19. **Balakrishnan L, Bambara RA**. 2013. Okazaki fragment metabolism. *Cold Spring Harb Perspect Biol* **5**: a010173.
20. **Nick McElhinny SA, Watts BE, Kumar D, Watt DL**, et al. 2010. Abundant ribonucleotide incorporation into DNA by yeast replicative polymerases. *Proc Natl Acad Sci USA* **107**: 4949–54.
21. **Reijns MAM, Rabe B, Rigby RE, Mill P**, et al. 2012. Enzymatic removal of ribonucleotides from DNA is essential for mammalian genome integrity and development. *Cell* **149**: 1008–22.
22. **Williams JS, Kunkel TA**. 2014. Ribonucleotides in DNA: origins, repair and consequences. *DNA Repair (Amst)* **19**: 27–37.
23. **Sparks JL, Chon H, Cerritelli SM, Kunkel TA**, et al. 2012. RNase H2-initiated ribonucleotide excision repair. *Mol Cell* **47**: 980–6.
24. **Lujan SA, Williams JS, Clausen AR, Clark AB**, et al. 2013. Ribonucleotides are signals for mismatch repair of leading-strand replication errors. *Mol Cell* **50**: 437–43.
25. **Czajkowsky DM, Liu J, Hamlin JL, Shao Z**. 2008. DNA combing reveals intrinsic temporal disorder in the replication of yeast chromosome VI. *J. Mol. Biol.* **375**: 12–9.
26. **Kaykov A, Nurse P**. 2015. The spatial and temporal organization of origin firing during the S-phase of fission yeast. *Genome Res* **25**: 391–401.
27. **Raghuraman MK, Winzeler EA, Collingwood D, Hunt S**, et al. 2001. Replication dynamics of the yeast genome. *Science* **294**: 115–21.
28. **Wyrick JJ, Aparicio JG, Chen T, Barnett JD**, et al. 2001. Genome-wide distribution of ORC and MCM proteins in *S. cerevisiae*: high-resolution mapping of replication origins. *Science* **294**: 2357–60.
29. **Yabuki N, Terashima H, Kitada K**. 2002. Mapping of early firing origins on a replication profile of budding yeast. *Genes Cells* **7**: 781–9.
30. **Feng W, Collingwood D, Boeck ME, Fox LA**, et al. 2006. Genomic mapping of single-stranded DNA in hydroxyurea-challenged yeasts identifies origins of replication. *Nat Cell Biol* **8**: 148–55.
31. **Müller CA, Hawkins M, Retkute R, Malla S**, et al. 2014. The dynamics of genome replication using deep sequencing. *Nucleic Acids Res* **42**: e3.
32. **Friedman KL, Brewer BJ, Fangman WL**. 1997. Replication profile of *Saccharomyces cerevisiae* chromosome VI. *Genes Cells* **2**: 667–78.
33. **Yamashita M, Hori Y, Shinomiya T, Obuse C**, et al. 1997. The efficiency and timing of initiation of replication of multiple replicons of *Saccharomyces cerevisiae* chromosome VI. *Genes Cells* **2**: 655–65.
34. **Cotobal C, Segurado M, Antequera F**. 2010. Structural diversity and dynamics of genomic replication origins in *Schizosaccharomyces pombe*. *EMBO J* **29**: 934–42.
35. **Segurado M, de Luis A, Antequera F**. 2003. Genome-wide distribution of DNA replication origins at A+T-rich islands in *Schizosaccharomyces pombe*. *EMBO Rep* **4**: 1048–53.
36. **Mojardín L, Vázquez E, Antequera F**. 2013. Specification of DNA replication origins and genomic base composition in fission yeasts. *J. Mol. Biol.* **425**: 4706–13.
37. **Heichinger C, Penkett CJ, Bähler J, Nurse P**. 2006. Genome-wide characterization of fission yeast DNA replication origins. *EMBO J* **25**: 5171–9.
38. **Hayashi M, Katou Y, Itoh T, Tazumi A**, et al. 2007. Genome-wide localization of pre-RC sites and identification of replication origins in fission yeast. *EMBO J* **26**: 1327–39.
39. **Xu J, Yanagisawa Y, Tsankov AM, Hart C**, et al. 2012. Genome-wide identification and characterization of replication origins by deep sequencing. *Genome Biol* **13**: R27.
40. **Lee JK, Moon KY, Jiang Y, Hurwitz J**. 2001. The *Schizosaccharomyces pombe* origin recognition complex interacts with multiple AT-rich regions of the replication origin DNA by means of the AT-hook domains of the spOrc4 protein. *Proc Natl Acad Sci USA* **98**: 13589–94.
41. **Hall MA, Shundrovsky A, Bai L, Fulbright RM**, et al. 2009. High-resolution dynamic mapping of histone-DNA interactions in a nucleosome. *Nat Struct Mol Biol* **16**: 124–9.
42. **Washietl S, Machné R, Goldman N**. 2008. Evolutionary footprints of nucleosome positions in yeast. *Trends Genet* **24**: 583–7.
43. **Prendergast JGD, Semple CAM**. 2011. Widespread signatures of recent selection linked to nucleosome positioning in the human lineage. *Genome Res* **21**: 1777–87.
44. **Sasaki S, Mello CC, Shimada A, Nakatani Y**, et al. 2009. Chromatin-associated periodicity in genetic variation downstream of transcriptional start sites. *Science* **323**: 401–4.

45. **Chen K, Meng Q, Ma L, Liu Q**, et al. 2008. A novel DNA sequence periodicity decodes nucleosome positioning. *Nucleic Acids Res* **36**: 6228–36.
46. **Moyle-Heyrman G, Zaichuk T, Xi L, Zhang Q**, et al. 2013. Chemical map of *Schizosaccharomyces pombe* reveals species-specific features in nucleosome positioning. *Proc Natl Acad Sci USA* **110**: 20158–63.
47. **Tillo D, Hughes TR**. 2009. G+C content dominates intrinsic nucleosome occupancy. *BMC Bioinformatics* **10**: 442.
48. **Quintales L, Soriano I, Vázquez E, Segurado M**, et al. 2015. A species-specific nucleosomal signature defines a periodic distribution of amino acids in proteins. *Open Biol* **5**: 140218.
49. **Soriano I, Morafraile EC, Vázquez E, Antequera F**, et al. 2014. Different nucleosomal architectures at early and late replicating origins in *Saccharomyces cerevisiae*. *BMC Genomics* **15**: 791.